Chitosan crosslinked flat scaffolds for peripheral nerve regeneration

Chitosan Crosslinked Flat Scaffolds for Peripheral Nerve Regeneration.

F. Fregnan[1], E. Ciglieri[1a], P. Tos[2], A. Crosio[2], G. Ciardelli[3], F. Ruini[3], C. Tonda-Turo[3], S. Geuna[1], S. Raimondo[1]

[1] Department of Clinical and Biological Sciences, and Cavalieri Ottolenghi Neuroscience Institute, University of Turin, Regione Gonzole 10,10043, Orbassano, Italy

[2] Reconstructive Microsurgery, Orthopedics Department, Trauma Center Hospital (CTO), Via Zuretti 29, 10100, Turin, Italy

[3]Department of Mechanical and Aerospace Engineering, Politecnico di Torino, Corso Duca degli Abruzzi 24, 10129, Torino, Italy

Permanent address

[a]Department of Veterinary Sciences, University of Turin, Largo Braccini 2, 10095 Grugliasco TO Italy.

Corresponding author:
Stefania Raimondo,
Department of Clinical and Biological Science, University of Turin,
Regione Gonzole 10,
10043 Orbassano (TO)
Tel +39 011 670 5433, fax +39 011 9038639,
E-mail stefania.raimondo@unito.it

Abstract

Chitosan (CS) has been widely used in a variety of biomedical applications, including peripheral nerve repair, due to its excellent biocompatibility, biodegradability, readily availability and antibacterial activity. In this study, CS flat membranes, crosslinked with dibasic sodium phosphate (DSP) alone (CS/DSP) or in association with the γ-glycidoxypropyltrimethoxysilane (CS/GPTMS_DSP), were fabricated with a solvent casting technique. The constituent ratio of crosslinking agents and CS were previously selected to obtain a composite material having both adequate mechanical properties and high biocompatibility.

In vitro cytotoxicity tests showed that both CS membranes allowed cell survival and proliferation. Moreover, CS/GPTMS_DSP membranes promoted cell adhesion, induced Schwann cell-like morphology and supported neurite outgrowth from dorsal root ganglia explants.

Preliminary in vivo tests carried out on both types of nerve scaffolds (CS/DSP and CS/GPTMS_DSP membranes) demonstrated their potential for: (i) protecting, as a membrane, the site of nerve crush or repair by end-to-end surgery and avoiding post-operative nerve adhesion; (ii) bridging, as a conduit, the two nerve stumps after a severe peripheral nerve lesion with substance loss.

A 1cm gap on rat median nerve was repaired using CS/DSP and CS/GPTMS_DSP conduits to further investigate their ability to induce nerve regeneration in vivo. CS/GPTMS_DSP tubes resulted to be more fragile during suturing and, along a 12-week post-operative lapse of time, they detached from the distal nerve stump. On the contrary CS/DSP conduits promoted nerve fiber regeneration and functional recovery, leading to an outcome comparable to median nerve repaired by autograft.

Key words: Peripheral nerve repair; regeneration; tubulization; chitosan; Schwann cells.

1. Introduction

Peripheral nerve traumas due to car crashes, sport and military injuries [1] are reported to affect, annually, more than one million people worldwide.

The possibility to regain nerve function is dependent on the severity of the damage suffered. Spontaneous recovery is possible only if the continuity of the nerve is maintained. In case of complete nerve transection, a surgery is required for re-establishing a continuity between the proximal and the distal stump. Autologous nerve grafts (autograft) is the "gold standard" technique for repairing peripheral nerve defects and it consists in the use of healthy nerve fragment of sensory origin (usually the sural nerve) for bridging the gap [2].

However, this practice presents some disadvantages: it requires an additional incision for removing the healthy sensory nerve, leading to a residue sensory deficit; yet, graft material is limited especially in case of an extended nerve lesion. As an alternative, a variety of biomaterials for nerve reconstruction has been developed [3,4]. In particular, chitosan (CS), as a natural polysaccharide, has recently attracted more and more attention due to its good biocompatibility, biodegradability, non-toxicity, readily availability and unique physicochemical properties [5,6].

Recent in vitro studies revealed the suitability of CS membranes as substrate for survival and oriented Schwann cell (SC) growth [7] as well as survival and differentiation of neuronal cells [8,9].

CS-based bioengineering scaffolds have been widely used for neural repair in different animal models [10]. CS-based nerve conduits, alone or in combination with other biomaterials, have been found to bridge efficiently peripheral nerve defects [11,12]. Yet, CS nerve guides supplied with the introduction of a longitudinal CS membranes were used to reconstruct 10-mm sciatic nerve defects in adult healthy and diabetic rats, demonstrating an enhancement in functional and morphological nerve regeneration [13].

Successful nerve regeneration of long gap has also been reported when CS surface was enriched with polylysine and gelatin to increase cell adhesion [14,15] or functionalized with polyglycolic acid [16].

Because pure CS is brittle and degrades rapidly [17,18], improved technologies and different crosslinking methods have been developed to overcome the poor mechanical strength of CS nerve guide channel under physiological conditions, which is one of the main factors limiting the CS use in clinical application for neural repair until now [19].

In the present work, dibasic sodium phosphate (DSP) and γ-glycidoxypropyltrimethoxysilane - DSP (GPTMS _DSP) crosslinked CS flat membranes, previously characterized in terms of physicochemical, thermal, morphological, mechanical properties [20], were evaluated in terms of biological properties using in vitro and in vivo tests.

In vitro studies on RTh-IN2ST cells were performed on degradable CS based flat membranes to evaluate biocompatibility and to ensure their potential applicability as nerve repair conduits. In addition, CS flat membranes and conduits were tested in an in vivo model of rat median nerve repair. The outcome of nerve reconstruction was assessed at 12 weeks post-implantation through a combination of functional assessment, histological and morphometrical investigation.

2. Methods

2.1 Membranes preparation

CS (medium molecular weight, 75%-85% deacetylation degree, Sigma Aldrich) was dissolved in acetic acid solution 0.5M at room temperature by continuous stirring to obtain a 2.5 % (w/v) solution. Crosslinked membranes were prepared according to the method previously described by Rnimi and colleagues [20]. In brief:

I. DSP-crosslinked samples (CS/DSP) were obtained by adding DSP 1M (one drop per second) to the CS solution with a concentration of 7.5 % v/v with respect to the neutral polymer solution volume. The mixed solution was kept under stirring at roomtemperature for about 10 minutes.

II. GPTMS_DSP crosslinked samples (CS/GPTMS_DSP) were obtained adding GPTMS (50% w/w) to the CS solution. The resulting CS/GPTMS solution was kept under stirring for 1 hour, followed by the dropwise addition (one drop per second) of DSP 1M (concentration 7.5 % v/v) and maintained under moderate stirring for 10 minutes.

Finally, 10 ml of each solution (CS/DSP and CS/GPTMS_DSP) was poured into 6 cm Petri dishes and air-dried for 48 h to obtain flat membranes. All crosslinked dried samples were dipped into deionizedlised water for 10 minutes and then the water pH values were measured to evaluate the presence of acidic residues.

Tensile test were performed by the authors, on CS/DSP and CS/GPTMS_DSP membranes, both in dry and in wet conditions [20].

2.2 In vitro cell tests on CS based membranes

In vitro cell tests were performed using RT0-D6P2T, a rat basonioma cell line (ATCC- catalog number CRL-1760). Cytotoxicity test was carried out on both CS/DSP and CS/GPTMS_DSP while, RT0-D6P2T adhesion, proliferation and gene expression were evaluated on CS/GPTMS_DSP due to the
k

higher mechanical stability of the biomaterial under physiological condition and because they were considered as “the worst case” (biomaterials employed for CS/GPTMS_DSP fabrication were the same of CS/DSP supplemented with GPTMS). Neurite outgrowth of dorsal root ganglia (DRG) cultured on CS/GPTMS_DSP was then examined by confocal laser microscopy.

2.2.1 -Cytotoxicity study on CS/GPTMS_DSP and CS/DSP

The effect of the CS based material extracts was studied on RT4-D6P2T. CS/DSP and CS/GPTMS_DSP samples were sterilized with a 20 minutes exposure to ultraviolet (UV) irradiation (UV lamp, wavelength 254 nm; Technoscientific Co., El- Haram Giza - Egypt). Material extracts were prepared by incubating both crosslinked CS based membranes in Dulbecco’s Modified Eagle Medium (DMEM, Sigma Aldrich) supplemented with 100 U/ml penicillin (Sigma), 0.1 mg/ml streptomycin (Sigma), 1 mM sodiumpyruvate (Sigma), 4 mM L-glutamine (Sigma) and 10% heat-inactivated fetal bovine serum (FBS; all from Invitrogen) and stored at 37 °C in a humidified atmosphere of 5% CO 2 for 13 days. As control media, samples of culture medium were maintained in the same conditions of CS/DSP and CS/GPTMS_DSP samples and then collected after 13 days. Then, proliferation assay on the cell line was carried out using collected media. In details, RT4-D6P2T cells were seeded and cultivated in the previous prepared extract media, at a density of $2x10^3$ cells/cm^2 on Petri dishes. After 2, 3, 5 and 7 days in vitro (DIV), cells were trypsinized and counted in a Burker’s hemocytometer chamber. Experiments were performed as technical triplicates. The counts obtained from assays were analyzed, averaged and expressed as logarithmic scale of viable cells/mm^2 ± SD.

2.2.2 -Cell adhesion on CS/GPTMS_DSP membranes

Immunocytochemistry analysis was performed to qualitatively evaluate cell adhesion and morphology. RTd-DkP2T were seeded at a density of 1.05×10^4/cm^2 on membranes and control glass slides. After 24 hours of culture, culture medium was removed, substrates with attached cells were rinsed with PBS and fixed by the addition of 4% paraformaldehyde solution (PAF; Sigma-Aldrich). After 20 min the PAF was removed and each plate was washed with PBS. Fixed cells were permeabilized with 0.1% Triton X-100 and blocked with 1% Normal goat serum in 0.01M PBS (pH 7.4) for 1 h at room temperature. F-actin was detected using TRITC-conjugated phalloidin diluted 1:1000 in blocking solution (Chemicon-Millipore) by 1 h incubation at room temperature following three wash steps of 5 min each. Vinculin was detected by overnight incubation with vinculin monoclonal antibody (Millipore) diluted 1:200 in PBS followed by 1-h incubation with goat-anti-mouse Alexa 488 secondary antibody (Invitrogen) diluted 1:200 in PBS.

A quantitative evaluation of the morphology of the cells plated on different substrates was conducted, taking into account the flattened or elongated cell shape. The value of flattened or elongated cells was expressed as a percentage of total evaluated cells in each experimental group. All the fluorescently-labeled cells were examined under a LSM 510 confocal laser microscopy system (Zeiss, Jena), which incorporates two lasers (argon and He/Ne) and is equipped with an inverted Axiovert 100 M microscope.

2.2.3 -Proliferation assay on CS/GPTMS_DSP membranes

RTd-DkP2T cells were seeded in DMEM containing 10% FBS, at a density of 2.5×10^3 cells/cm^2 on both CS/GPTMS_DkP and glass control plates (control). After 1, 3 and 4 DIV, culture medium was removed, substrates with attached cells were rinsed with PBS and fixed by the addition of 4% PAF. After 20 min, PAF was removed and each plate was washed with PBS. RTd-DkP2T cells were stained with 1% crystal violet (a deep purple nucleic acid stain) solution in 200 mM boric solution (pH 9) for

10 min at room temperature. Cells were photographed at DFC 320 Leica microscope and 30 images were taken at a low magnification (10X) for each sample. The images were then acquired through the program Image Manager IM50 (Leica). The counts obtained from proliferation assay were analyzed, averaged and expressed as logarithmic scale of viable cells/cm² ± SD.

2.2.4- Real Time Reverse-Transcriptase-Polymerase-Chain-Reaction (Real Time RT- PCR) analysis on CS/GPTMS_DSP.

RT6-D6P2T cells were cultured in DMEM containing 10% FBS on glass control plates and CS/GPTMS_DSP flat membranes and were allowed to reach confluence. The total RNA was isolated from the confluent culture by extraction with TRIzol (Invitrogen). The RNA concentration was quantified by measuring the absorbance at 260/280 nm. The total RNA (1 µg per sample) was reverse-transcribed in a reaction volume of 25 µl with 7.5 mM of random hexamers (Thermo Scientific). Each reaction consisted of cDNA synthesis buffer (50×10^{-3} M Tris-HCl, pH 8.3, 75×10^{-3} M, KCl, 3×10^{-3} M $MgCl_2$), 1 mM deoxynucleoside triphosphate (dNTP), Thermo Scientific), 1.3 U/µl ribonuclease inhibitor (RNAsin, RiboLock Thermo Scientific) and 8 U/µl Moloney murine leukaemia virus (M-MLV) reverse transcriptase (RevertAid Thermo Scientific). Samples were then exposed to a first cycle: 25°C for 10 min, 42°C for 90 min and 90°C for 10 min. Specific primers designed to amplify B cell lymphoma 2 (Bcl2)-associated X protein (BAX), Bcl2 (two proteins involved in the cascade of caspases, which regulates cellular apoptosis), superoxide dismutase (SOD, an important antioxidant defense in nearly all living cells exposed to oxygen) and mammalian target of rapamycin (mTor, a protein encoded by the MTOR gene involved in the regulation of cell growth, cell proliferation, cell motility, cell survival, protein synthesis, and transcription) are listed below.

Bax Forward Sequence- TTGCTGATGGCAACTTCAAC; Reverse Sequence-

GATCAGCTCGGGCACTTTAG. **Bcl2**: Forward Sequence- GCATCTGCACACCTGGATC; Reverse Sequence- GGGCCATAEAGTTCCACAAAGG. **Sod**: Forward Sequence- GAGGCCATCCCTTATCCAAG ; Reverse Sequence- GATGCCACAGCCCAACC. **m-TOR**: Forward Sequence- GCTCTCTGACAAGGAGAGAG; Reverse Sequence- GCCTCTCGACAAGGAGATAG.**IRC**: Forward Sequence- CCACCAAGAAGGTCAACAGG; Reverse Sequence- CCCATCACACCCAAGAACAAG. **TBP**: Forward Sequence- GATCAAACCCAGAATTGTCTCTC; Reverse Sequence- GGGGTAGATGTTTTCAAATGCTTC

For normalization to multiple housekeeping genes, ubiquitin gene C (UBC) and TATA-binding protein (TBP) were used. The reaction mixture of PCR included 7.5µg forward and reverse primers, 12.5 µl SYBR Green (Life Technologies) and 5 µl cDNA. The PCR conditions were as following: initial step at 95°C for 25 s, then 40 cycles at 60 °C for 35 s, and 60 °C for 1 min. The results were obtained from three independent experiments.

2.2.5- Total protein extraction, and western blot

Total proteins were extracted by solubilizing cells in boiling Laemmli buffer (2.5% SDS and 0.125 M Tris-HCl pH 6.8), followed by 3 min at 100°C. Protein concentration was determined by the BCA method, and equal amounts of protein (denaturated at 100°C in 240 mM 2-mercapto ethanol and 18% glycerol) were loaded onto each lane, separated by SDS-PAGE, transferred to a HybondTM C Extra membrane and blocked for 1 h at 37 °C in 1× TBST (150 mM NaCl, 10 mM Tris–HCl (pH 7.4), and 0.1% Tween) plus 5% non-fat milk. Membranes were incubated overnight at 4 °C in primary antibodies diluted in TBST plus 1% non-fat milk. The day after, they were rinsed four times with TBST for 5 min each at room temperature and incubated for 1 h at room temperature with peroxidase-linked secondary antibody (diluted in TBST plus 1% non-fat milk). Membranes were washed 4 times, 5 min each, with

TBST at room temperature, and specific binding was detected by the enhanced chemiluminescence ECL-system (Amersham Biosciences) using HyperFilm™ (Amersham Biosciences).

Primary and secondary antibodies used are: rabbit polyclonal anti-BrI2 (1:500, sc-492, Santa Cruz Biotechnology, Santa Cruz, CA, USA); mouse monoclonal anti-actin (1:4000, #A5316, Sigma); horseradish peroxidase–linked donkey anti-rabbit secondary antibody (1:10.000, Amersham Biosciences), sheep anti-mouse secondary antibody (1:100.000, Amersham Biosciences).

2.2.6-Neurite outgrowth assay on CS/GPTMS_DSP

DRGs explants were harvested from adult female Wistar rats, weighting approximately 250 g, reduced and maintained in Ham's nutrient mixture F12 (Gibco) for 1 hour under sterile conditions. Rats were sacrificed by a lethal i.p. injection of tiletamine + zolezil, according with the local Ethics Committee and the European Communities Council Directive 2010/63/EU. Adequate measures were taken to minimize pain and discomfort taking into account human endpoints for animal suffering and distress. DRG explants were cultured onto matrigel-coated coverslips (BD Biosciences) and CS/GPTMS_DSP flat membranes and incubated at 37 °C for 1 hour. The matrigel was diluted 1:1 in the culture medium. Explants were maintained for 4 days in defined serum-free medium (SFM) at 37 °C, with 5% CO 2, supplemented with 50 ng/ml of NGF. After 4 days, explants were fixed with 4% PAF for 15 minutes at room temperature. For immunohistochemistry, briefly, the specimens were incubated overnight in a solution containing both anti-neurofilament-200kDa (monoclonal mouse, 1:200, Sigma), and anti-peripherin (polyclonal rabbit, 1:1000, Chemicon International) primary antibodies. After washing in PBS, double immunolabeling was carried out by incubating sections for 1 h in a solution containing two secondary antibodies: anti-rabbit IgG-Cy3 (Jackson Immunoresearch Laboratory) and anti-mouse IgG Alexa-Fluor-488-conjugated (Molecular Probes). All samples were observed with a LSM 510

confocal laser microscopy system (Zeiss, Jena), which incorporates two lasers (argon and HeNe) and is equipped with an inverted Axiovert 100 M microscope.

2.3 In vivo tests on CS/GPTMS_DSP and CS/DSP

All procedures were approved by the Bioethics Committee of the University of Torino, by the Institutional Animal Care and Use Committee of the University of Torino, and by the Italian Ministry of Health, in accordance with the European Communities Council (Directive 2010/63/EU).

2.3.1 -Animals and surgery

In vivo preliminary analysis were performed under general anesthesia on 2 adults female Wistar rats, weighing approximately 250 g, in order to evaluate healthiness, sutureability and the possibility of their use for peripheral nerve surgery. Before using CS membranes were immersed in PBS solution for 5 minutes and showed a uniform thickness in the range of 90-130 μm. In the first rat, the CS membrane was used to wrap crushed median nerve and was closed with a suture point (Figure.1 A,B). In the second rat, the CS membranes were rolled up and glued with biomedical cyanoacrylate glue to obtain 1 cm long conduit (Figure.1 C-F). Median nerves were transected, 5 mm of median nerve was removed and CS/DSP and CS/GPTMS_DSP tubes were sutured bridging the two nerve stumps (Figure.1 G,H) that were inserted 2mm inside the conduit. Animals were sacrificed immediately after surgery.

Afterwards, nerve regeneration assays were carried out on 12 adult female Wistar rats, weighing approximately 250 g, with both CS/DSP and CS/GPTMS_DSP membranes, rolled up and glued as described above, used as conduits for median nerve repair. The animals were divided by three experimental groups of 4 animals each. In two groups, the median nerve was transected and repaired with CS/DSP or CS/GPTMS_DSP conduits. Median nerve repaired with nerve autograft was used as control. The surgery procedure was previously described by Tos and collegues [21]. The autograft and

the conduit were sutured using three or four stitches of 9–0 monofilament nylon for each stump. In order to prevent interferences with the grasping test device during testing due to the use of the contralateral forepaw, the contra-lateral median nerve was transected at the middle third of the brachium and its proximal stump was sutured in the pectoralis major muscle to avoid spontaneous reinnervation [22]. After 12-weeks post-operative, rats were sacrificed and regenerated nerves analysed.

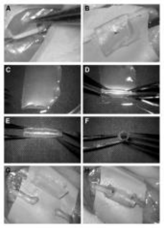

Figure. 1. Preliminary in vivo results. *A,B: CS membrane used to wrap crushed rat median nerve. C-H: CS membrane enrolled to prepare a conduit for repairing severe median nerve lesions. C: CS membrane was immersed in PBS solution; D-F: CS membrane was rolled and glued with a cyanoacrylate glue to obtain a tube; G,H: CS conduit immediately before and after implantation for the repair of a rat median nerve.*

2.3.2- Postoperative assessment of functional recovery

Grasping test sessions were carried out every 3 weeks until week 12. Grasping test was performed following the same procedure previously described [22] using the BS-GRIP Grip Meter (Bioskogical Instruments, Varese, Italy). The test is carried out by holding the rat by the tail and lowering it towards the device and then, when the animal grips the grid, pulling it upward until it loses its grip. When the median nerve function is impaired, the animal's paw approaches the grid in complete finger extension. The balance records the maximum weight that the animal manages to hold up before losing the grip. Each animal was tested three times and the average value was recorded. Since assessment of animal welfare was one of the main objectives of this study, a careful daily animal surveillance was adopted for passive and active movement, auto-mutilation and joint contracture, especially during early post-operative times.

2.3.3- Immunohistochemistry and confocal laser microscopy

From all animals, the entire conduit, with regenerating fibers inside, was frozen, cut and analyzed with immunofluorescence at confocal laser microscopy. Series of 8–10 µm-thick longitudinal sections were cut by a Cryostat (Leica Microsystems, Wetzlar, Germany). Sections were then incubated overnight in a solution containing anti-neurofilament-200kDa primary antibody (monoclonal, mouse, which recognizes the 200 kDa subunit of neurofilaments, dilution 1:200, Sigma) and then, after washing in PBS, incubated for 1 hour in a solution containing Alexa488-conjugated anti-mouse IgG (dilution 1:200, Life technologies). The sections were finally mounted with a Dako fluorescent mounting medium and analyzed by a LSM 510 confocal laser microscopy system (Zeiss, Jena, Germany).

2.3.4- Resin embedding and electron microscopy

After the 12-week follow-up time, animals were euthanized and the nerve segment distal to the conduit was collected, fixed, and prepared for design-based stereological analysis of myelinated nerve fibers and for electron microscopy. Nerve samples were fixed by immediate immersion in 2.5% purified glutaraldehyde and 0.1% saccarose in 0.1 M Sorensen phosphate buffer for 6–8 hours. Specimens were then washed in a solution containing 1.5% saccarose in 0.1 M Sorensen phosphate buffer, post-fixed in 1% osmium tetroxide, dehydrated and embedded in resin. From each nerve, series of semi-thin transverse sections (2.5-μm thickness) were cut starting from the distal stump of each median nerve specimen, using an Ultracut UCT ultramicrotome (Leica Microsystems, Wetzlar, Germany) and stained using Toluidine blue for high resolution light microscopy examination and design-based stereology. For transmission electron microscopy, ultrathin sections (50–90-nm thick) were cut using the same ultramicrotome and stained with saturated aqueous solution of uranyl acetate and lead citrate. Ultra-thin sections were analyzed using a JEM-1010 transmission electron microscope (JEOL, Tokyo, Japan).

2.3.5–Design-based quantitative morphology of nerve fiber regeneration

In each nerve repaired with autograft or CS/DSP conduit, design-based stereological analysis was carried out using one randomly selected toluidine blue stained semithin sections. A DM4000B microscope equipped with a DFC320 digital camera and an IM50 image manager system (Leica Microsystems, Wetzlar, Germany) was used for stereology. The final magnification was 6600X enabling accurate identification and morphometrical analysis of myelinated nerve fibers. One semi-thin section from each nerve was randomly selected and the total cross-sectional area of the nerve was measured. The sample of fibers in each nerve was then randomly selected using a previously described stereological method [25]. Two-dimensional disector probes were also used to select an unbiased representative sample of myelinated nerve fibers. Fiber number was calculated, both fiber and axon

axes were measured and the circle-fitting diameter of fiber (D) and axon (d) were calculated. These data were used to calculate myelin thickness [(D−d)/2], and the g-ratio (D/d).

2.4 Statistics

For in vitro experiments, data were expressed as mean ± SEM. Statistical analysis was carried out using single-factor analysis of variance (ANOVA) post hoc Bonferroni. Values of *p≤0.05, **p≤0.01, ***p≤0.001 were considered as statistically significant. For in vivo experiments data were expressed as mean ± SD Statistical analysis was carried out using Two-Sample t-Test. Values of *p≤0.05, **p≤0.01, ***p≤0.001.

3. Results

3.1 In vitro cell tests on CS based samples

3.1.1 - Cytotoxicity study on CS/GPTMS_DSP and CS/DSP

The effect of the CS based material extracts was studied by RTH-D4P2T proliferation assay counting the number of proliferating cells after 2, 3, 5 and 7 DIV (Figure 2). RTH-D4P2T treated with extracts of CS/DSP and CS/GPTMS_DSP showed no cytotoxic effects since no significant differences in cell number were detected between these two culture conditions and the control.

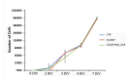

Figure. 2. Evaluation of the effect of dissolution products. *Logarithmic scale of RT4-D6P2T cells/seed proliferated after 1, 3, 5 and 7 DIV seeded in control, CS/DSP and CS/GPTMS_DSP extract media.*

3.1.2 -Cell adhesion on CS/GPTMS_DSP membranes

RT4-D6P2T cells were seeded on CS/GPTMS_DSP and on control glass; immunocytochemistry analysis was performed after 24 hours of culture to qualitatively evaluate cell adhesion and morphology. In order to obtain a more detailed evaluation of cell adhesion, the actin cytoskeleton and focal adhesion complex were stained using TRITC-conjugated phalloidin and anti-vinculin antibody, respectively. RT4-D6P2T cells interacted and integrated well with CS/GPTMS_DSP substrate. Differences in morphology and size were observed when RT4-D6P2T cells were cultured on control glass and CS/GPTMS_DSP (Figure 3). Cells on control glass displayed a higher size; they were also more spread without particular orientation of the actin cytoskeleton (Figure 3A and C). Cells cultured on CS/GPTMS_DSP displayed a more elongated morphology characterized by a typical oval-shaped cell body with long extensions, giving an overall spindle shape that is typical of SCs (Figure 3B and D).

The analysis of the morphology of these cells plated on different substrates showed that the 68% of cells plated on control substrates (glass) presented a flattened form, similarly to fibroblasts, and only

32% as elongated shape similarly to SCs. By contrast, 84% of the cells cultured on CS/GPTMS_DSP that presented the SC-like elongated shape.

Vinculin immunostaining was performed to visualize the exact location of focal adhesion sites. Vinculin-positive sites were observed on cells seeded both on control and CS/GPTMS_DSP, but with different distribution. CS/GPTMS_DSP membranes presented cells with a higher accumulation of vinculin around the nucleus (Figure 3F) while protein accumulation at the edges of cells was mainly showed in control (Figure 3E).

3.1.3- Proliferation assay on CS/GPTMS_DSP membranes

Proliferation assay was performed on CS/GPTMS_DSP samples (Figure 3G). RT4-D6P2T cells were cultured on both CS/GPTMS_DSP and glass plates (control). The number of proliferating cells was then counted after 1, 3 and 4 DIV.

RT4-D6P2T cells seeded on CS/GPTMS_DSP showed lower proliferation rate and significant differences in cells numbers were detected in this culture conditions after 3 DIV (**p<0.01) and 4 DIV (***p<0.001), in comparison to positive control. Yet, it was possible to observe a constant increase of cell number on CS/GPTMS_DSP samples at each time point.

3.1.4- Gene and protein expression of RT4-D6P2T cultured on CS/GPTMS_DSP samples.

Bax, Bcl2, mTOR and SOD mRNA expression changes were evaluated to study pro-apoptotic and cell survival signaling after 3 and 6 days of culture of RT4-D6P2T cells on CS/GPTMS_DSP samples.

The relative values of BAX, mTOR and SOD mRNA expression were not significantly different when comparing CS/GPTMS_DSP with control condition, both after 3 and 6 days of culture. (Data not shown). By contrast, significant difference in the Bcl2 mRNA expression was shown in after 3 days of

culture (*p<0.05) compared to the control, although this difference was no more observed after 6 days (Figure 3H).

The same pattern of expression was detected at the protein level; the decreased protein expression of Bcl2, after three days of culture of the RT4-D6P2T cells on chitosan membranes, undergoes a clear increase after six days of culture, although still lower than control values. (Figure 3I).

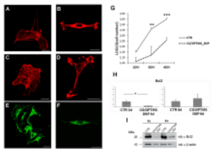

Figure. 3. Cell adhesion assessment. *Confocal fluorescence microscopy images of RT4-D6P2T cells cultured on control glass (A, C, E) and CS/GPTMS_DSP (B, D, F) after 24 hours of culture. Phalloidin (A, B, C, D) and anti-vinculin (E, F) staining. Scale bar 20 µm.* ***Cell proliferation assay.*** *RT4-D6P2T proliferation ratio after 1, 3 and 4 DIV on glass plates (control) and on CS/GPTMS_DSP membranes. RT4-D6P2T significant differences between CS/GPTMS_DSP substrates and control samples were observed (**p<0.01; ***p<0.001) (G).* ***Gene and protein expression analysis.*** *RT PCR expression profiles of Bcl2 messengers in RT4-D6P2T seeded respectively on control plates, and CS/GPTMS_DSP membranes after 3 and 6 days of culture (H). Significative difference between the biomaterial and control was observed for Bcl2 after 3 days of culture (*p<0.05). Western blot analysis for Bcl-2 protein expression of RT4-D6P2T cells cultured on glass plates and on CS/GPTMS_DSP membranes for 3 and 6 days. Anti- β-actin antibodies was used as control (I).*

3.1.5 -Neurite outgrowth assay on CS/GPTMS_DSP

DRG explant were harvested from adult female Wistar rats and cultured for 4 days on rastriged-coated coverslips and CS/GPTMS_DSP flat membranes. The cultures were fixed and immunostained for NF-200kDa (green) and peripherin (red) and then analyzed by laser confocal microscopy. A double labeling immunofluorescence revealed that both neuronal intermediate filament proteins were expressed by DRG neurons (Figure 4).

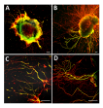

Figure 4. Ex vivo neuronal regrowth evaluation. *Representative immunostaining images of axonal outgrowth at 4 days after DRG explants culture on rastriged-coated coverslips (A, C) and CS/GPTMS_DSP flat membranes (B, D) using anti-NF-200kDa antibody (green) and anti-peripherin (red). Scale bar: 100 μm.*

3.2 In vivo preliminary analysis

In order to evaluate maneuverability for peripheral nerve surgery, flat membranes of CS/DSP and CS/GPTMS_DSP were tested in vivo in adult female Wistar rats.

Both membranes have to be immersed in PBS before use in order to make them softer. Surgeons can adapt size and shape of membranes depending on the size of the nerve and the lesion type and extent. They can be used to protect an injured nerve from adhesions (Figure 1Bi) or as conduit to bridge a nerve defect (Figure 1Bi). Both membranes resulted to have a good maneuverability after the PBS immersion

and they are easy to be cut with a scalpel, in order to give them the appropriate size, and they are easily rolled up and glued. CS/GFIMS_DSP resulted to be much more fragile.

3.3 In vivo tests with CS/GFIMS_DSP and CS/DSP conduits

3.3.1 -Postoperative assessment of functional recovery

In vivo nerve regeneration experiments were carried out with both CS/DSP and CS/GFIMS_DSP conduits. The resected median nerves of female Wistar rats were repaired by rolled-up and tube-shaped CS/DSP or CS/GFIMS_DSP membranes. Reversed autologous nerve graft (autograft) repair was used as control.

Figure 5 reports the post traumatic time course of functional recovery for rats treated using CS/DSP and autologous graft. In the group of CS/GFIMS_DSP conduits, functional recovery of finger flexor muscles did not occurred during all post-operative period. This showed to be due to the detachment of CS/GFIMS_DSP tubes from the distal nerve stump.

The function of finger flexor muscles innervated by the median nerve started to recover faster for autografts reaching a performance statistically different from CS/DSP at week-6 after lesion (*p<0.05). Functional recovery for CS/DSP started at week-6 and progressively increased. At week-9 and 12, no more significant differences were detectable between autograft and CS/DSP treatment.

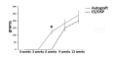

Figure 5. In vivo functional analysis. *Line graph reporting the post-traumatic time course of functional recovery as assessed by the gripping test. Values are mean ± standard deviation. Significant difference between CS/DSP and autograft- treated functional recovery was observed at 6 weeks (*p<0.05).*

3.3.2- Immunohistochemistry and confocal laser microscopy

Axonal regeneration was analysed by confocal laser microscopy on longitudinal nerve frozen sections after neurofilament staining (Figure 6). After 12-week post-injury, the middle segments of both CS/GPTMS_DSP and CS/DSP conduit displayed NF positive staining for axons, with a disordered and irregular orientation in the CS/GPTMS_DSP conduit (Figure 6A) and linearly oriented in CS/DSP conduit (Figure 6B).

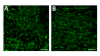

Figure 6. In vivo axonal regrowth evaluation. *Neurofilament staining on longitudinal sections at 12 weeks post-injury. CS/GPTMS_DSP were densely populated with axons. CS/GPTMS_DSP displayed axons that were highly-packed, irregularly oriented and disordered (A), while properly linearly aligned NF axons were found on CS/DSP (B). Scale-bar 100 µm.*

3.3.3- Light and transmission electron microscope analysis

Figure 7 shows high-resolution light and transmission electron microscope images of the distal rat median nerves injured, repaired with autograft or CS/DSP conduits and harvested at 12 weeks post-operation. Distal median nerves treated with CS/GPTMS_DSP were not harvested because conduits were found to be detached from the distal tutoring rats. Small myelinated axons and microfascicleties typical of regenerated nerve fibers were detected both on nerves repaired with autograft (Figure 7 A,C,E,G) and with CS/DSP conduit (Figure 7H,D,F,H) .

Moreover, transmission electron microscopy detected many small nerve fibers in early stages of myelinization (Figure 7E,F) as well as unmyelinated fibers (Figure 7G,H), in median nerves repaired both with CS-ISP conduit and with autograft.

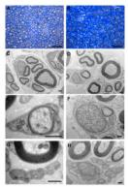

Figure 7. Morphological analysis. *Photomicrographs of semi-thin sections cut transversely to the main axis of median nerves repaired using autologous graft (A) and CS-ISP (B) 12 weeks post operation. Electron photomicrographs of median nerves repaired using autograft (C, D) and CS-ISP (E-H) regenerated nerves 12 weeks post operation. Scale bars: A,B: 20 μm; C, D, H = 1 μm; E, F, G=0.5 μm.*

3.3.4- Design-based quantitative morphology of nerve fiber regeneration

12-week post injury, design-based stereological analysis of regenerated median nerves repaired with CS/DSP tubes or autograft showed comparable results in terms of total number of myelinated fibers (autograft = 6916±1631; CS/DSP = 7249±613). Axon and fibers diameters and G-ratio was significantly lower (*p<0.05) in median nerves repaired with CS/DSP tubes when compared to autografts, while myelin thickness showed comparable results (Figure 8).

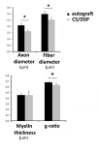

Figure 8. Morphometrical analysis of regenerating fibers. *Bar Graph representing stereological parameters of myelinated nerve fibers in regenerated median nerves 12-week post-injury,using autograft and CS/DSP tubes. Values are expressed as mean ± S.D. Significant differences between the datapreserved and the gold standard approach were observed for axon and fiber diameter, and for g-ratio (*p<0.05).*

4. Discussion

Applications of CS in tissue engineering is a very actual and evolving topic [1624]. This biomaterial is attractive not only for the high biocompatibility and biodegradability, but also for the antibacterial properties and the absence of immune responses.

However, physical and mechanical limitations of CS when it is associated with aqueous solution have to be carefully considered in order to apply it properly for regenerative purposes.

In this manuscript, CS was treated with crosslinking agents able to act on its chemical-physical and mechanical properties, namely γ-glycidoxypropyltrimethoxysilane (GPTMS), dibasic sodium phosphate (DSP) and a combination of GPTMS and DSP (GPTMS_DSP), as previously described by Raini and colleagues [20].

The presence of GPTMS showed that silicon agent was homogeneously distributed in the developed membranes and increased the water stability and the softness of CS/GPTMS_DSP membranes compared to CS/DSP samples.

Both CS/GPTMS_DSP and CS/DSP flat membranes were studied in vitro and in vivo for the implementation of CS-based nerve scaffolds.

First of all, the products of degradation of the CS membranes, both CS/DSP and CS/GPTMS_DSP, showed no negative effects on glial cell survival and proliferation.

Yet, proliferation analysis of glial cells seeded on CS/GPTMS_DSP membranes led to confirm that CS is capable to support glial cell proliferation [25] although delayed in comparison to positive control. This is attributable to the need for an initial adjustment to the new substrate. The need of adaptation of the cells to the substrate was demonstrated also by gene expression analysis of the anti-apoptotic gene Bcl2 that is significantly lower in cells grown for 3 days on CS/GPTMS_DSP, while the difference was no more detectable after 6 days.

The analysis of cell adhesion to the CS/GPTMS_DSP membrane showed that glial cells displayed a different morphology and actin and vinculin distribution, supporting the view that these cells have a higher migratory capacity on the biomaterial, a key requirement for the early stages of nerve regeneration [26]. The actin cytoskeleton is a highly dynamic network composed of actin polymers and a large variety of associated proteins. The function of the actin cytoskeleton is to mediate a variety of essential biological functions, including intracellular and extracellular movement and structural support. The orientation and distribution of actin filaments within a cell is, therefore, an important determinant of cellular shape, adhesion and motility [27].

The assessment of the interaction of neurons with the material represents a key preliminary step to evaluate, in vitro, the potential for neural regeneration. Explants of rat dorsal root ganglia (DRGs) are a valuable ex vivo model to observe the neuritic adaptation to different substrates [28]. In our research, adults DRGs were cultured on CS/GPTMS_DSP membranes and on glass, as control. After four days, a high neurite outgrowth, expressing protein markers of both young and mature axons, was appreciated on both substrates. Although quantitative analysis was not carried out, careful observation led to detect a greater sprouting and neurite extension on the CS substrate in comparison to control.

In preparation of in vivo experiments, a series of preliminary tests allowed us to evaluate the manoeuvrability of CS membranes. It was possible to establish the easy handling and the possibility to build, at the time of the surgery, a tube of specific size and shape depending on the extent of nerve damage, although it was evident that the CS/GPTMS_DSP is much more fragile in comparison with CS/DSP.

Both CS/DSP and CS/GPTMS_DSP conduits were used for bridging across 10-mm long rat median nerve defects, and the outcome at 12 weeks post-implantation was evaluated by functional, immunohistochemical and histological investigation. We observed that CS/GPTMS_DSP tubes were detached from the distal suturing site, due to excessive fragility, and thus no functional recovery

occurred. This result was confirmed by confocal laser microscopy which displayed very poor axonal regeneration with an irregular orientation inside CS/GPTMS_DSP conduits.

By contrast, CS/DSP conduit allowed functional recovery that started at week-6 and progressively increased reaching values similar to autografts already at week-9. The delayed functional recovery is justified by the different repair technique and it is line with the results obtained using other types of conduits [29].

Interestingly, morphological analysis showed microfascicolation typical of regenerated nerve fibers with small nerve fibers at different myelinization stages and unmyelinated fibers, though morphometrical analysis revealed that CS/DSP have, on average, smaller fibers than autograft.

5. Conclusion

In this work, we have selected a biomaterial, namely chitosan, because of its excellent biocompatibility, biodegradability, readily availability and antibacterial activity. Crosslinking process has provided chitosan with adequate mechanical properties for successful application in the field of peripheral nerve regeneration.

Our experiments showed that CS/DSP scaffolds promote peripheral nerve regeneration with an outcome close to that reached by nerve autografts which are generally considered as the gold standard for treating severe nerve defects. These newly developed nerve guides should thus be regarded as promising alternatives to traditional nerve autografts.

However, it could be foreseen that enrichment of chitosan scaffolds with filling materials conjugated with growth factors [30] might be able to further increase the effectiveness of the medical device. Yet, creation of a 3D inner structure, which simulate extracellular matrix, might also provide a further support to axons and glial cells [31,32,33]. Therefore, although the device that we propose is simple

and easy to apply during surgery, future experiments should clarify whether the functionalization of the crosslinked chitosan tubes can further increase the regenerative potential of the device.

Acknowledgements

This research was supported by Regione Piemonte - Poli di Innovazione - RICONBIVE project (number: 18K-3SSC).

The authors declare no conflict of interest.

References

1. Daly W, Yao L, Zeugolis D, Windebank A, Pandit A (2012) A biomaterials approach to peripheral nerve regeneration: bridging the peripheral nerve gap and enhancing functional recovery. J R Soc Interface 9: 202-221.
2. Gravvanis AI, Lavdas A, Papalois AE, Franceschini I, Tsoutsos DA, et al. (2005) Effect of genetically modified Schwann cells with increased motility in end-to-side nerve grafting. Microsurgery 25: 423-432.
3. J I-P, Jansen K, Gramsbergen A, Meek MF (2004) Transection of peripheral nerves, bridging strategies and effect evaluation. Biomaterials 25: 1583-1592.
4. Raimondo S, Fornaro M, Tos P, Battiston B, Giacobini-Robecchi MG, et al. (2011) Perspectives in regeneration and tissue engineering of peripheral nerves. Ann Anat 193: 334-340.
5. Hsu SH, Ho TT, Tseng TC (2012) Nanoparticle uptake and gene transfer efficiency for MSCs on chitosan and chitosan-hyaluronan substrates. Biomaterials 33: 3639-3650.
6. Busilacchi A, Gigante A, Mattioli-Belmonte M, Manzotti S, Muzzarelli RA (2013) Chitosan stabilizes platelet growth factors and modulates stem cell differentiation toward tissue regeneration. Carbohydr Polym 98: 665-676.
7. Yuan Y, Zhang P, Yang Y, Wang X, Gu X (2004) The interaction of Schwann cells with chitosan membranes and fibers in vitro. Biomaterials 25: 4273-4278.
8. Freier T, Koh HS, Kazazian K, Shoichet MS (2005) Controlling cell adhesion and degradation of chitosan films by N-acetylation. Biomaterials 26: 5872-5878.
9. Simoes MJ, Gartner A, Shirosaki Y, Gil da Costa RM, Cortez PP, et al. (2011) In vitro and in vivo chitosan membranes testing for peripheral nerve reconstruction. Acta Med Port 24: 43-52.
10. Gnavi S, Barwig C, Freier T, Haastert-Talini K, Grothe C, et al. (2013) The use of chitosan-based scaffolds to enhance regeneration in the nervous system. Int Rev Neurobiol 109: 1-62.
11. Xu H, Yan Y, Li S (2011) PDLLA/chondroitin sulfate/chitosan/NGF conduits for peripheral nerve regeneration. Biomaterials 32: 4506-4516.
12. Haastert-Talini K, Geuna S, Dahlin LB, Meyer C, Stenberg L, et al. (2013) Chitosan tubes of varying degrees of acetylation for bridging peripheral nerve defects. Biomaterials 34: 9886-9904.
13. Meyer C, Wrobel S, Raimondo S, Rochkind S, Heimann C, et al. (2016) Peripheral Nerve Regeneration Through Hydrogel-Enriched Chitosan Conduits Containing Engineered Schwann Cells for Drug Delivery. Cell Transplant 25: 159-182.
14. Mingyu C, Kai G, Jiamou L, Yandao G, Nanming Z, et al. (2004) Surface modification and characterization of chitosan film blended with poly-L-lysine. J Biomater Appl 19: 59-75.

15. Cheng M, Deng J, Yang F, Gong Y, Zhao N, et al. (2003) Study on physical properties and nerve cell affinity of composite films from chitosan and gelatin solutions. Biomaterials 24: 2871-2880.

16. Wang X, Hu W, Cao Y, Yao J, Wu J, et al. (2005) Dog sciatic nerve regeneration across a 30-mm defect bridged by a chitosan/PGA artificial nerve graft. Brain 128: 1897-1910.

17. Wang A, Ao Q, Wei Y, Gong K, Liu X, et al. (2007) Physical properties and biocompatibility of a porous chitosan-based fiber-reinforced conduit for nerve regeneration. Biotechnol Lett 29: 1697-1702.

18. Yang Y, Gu X, Tan R, Hu W, Wang X, et al. (2004) Fabrication and properties of a porous chitin/chitosan conduit for nerve regeneration. Biotechnol Lett 26: 1793-1797.

19. Ao Q, Fung CK, Tsui AY, Cai S, Zuo HC, et al. (2011) The regeneration of transected sciatic nerves of adult rats using chitosan nerve conduits seeded with bone marrow stromal cell-derived Schwann cells. Biomaterials 32: 787-796.

20. Ruini F, Tonda-Turo C, Chiono V, Ciardelli G (2015) Chitosan membranes for tissue engineering: comparison of different crosslinkers. Biomed Mater 10: 065002.

21. Tos P, Ronchi G, Nicolino S, Audisio C, Raimondo S, et al. (2008) Employment of the mouse median nerve model for the experimental assessment of peripheral nerve regeneration. J Neurosci Methods 169: 119-127.

22. Tos P, Ronchi G, Papalia I, Sallen V, Legagneux J, et al. (2009) Chapter 4: Methods and protocols in peripheral nerve regeneration experimental research: part I-experimental models. Int Rev Neurobiol 87: 47-79.

23. Kaplan S, Geuna S, Ronchi G, Ulkay MB, von Bartheld CS (2010) Calibration of the stereological estimation of the number of myelinated axons in the rat sciatic nerve: a multicenter study. J Neurosci Methods 187: 90-99.

24. Nastasescu OS, Popa IM, Verestiuc L, Butnaru M, Baran D (2008) [Scaffolds based on collagen and chitosan for post-burn tissue engineering]. Rev Med Chir Soc Med Nat Iasi 112: 547-553.

25. Li G, Zhao X, Zhao W, Zhang L, Wang C, et al. (2014) Porous chitosan scaffolds with surface micropatterning and inner porosity and their effects on Schwann cells. Biomaterials 35: 8503-8513.

26. Chen YY, McDonald D, Cheng C, Magnowski B, Durand J, et al. (2005) Axon and Schwann cell partnership during nerve regrowth. J Neuropathol Exp Neurol 64: 613-622.

27. Johnson HE, King SJ, Asokan SB, Rotty JD, Bear JE, et al. (2015) F-actin bundles direct the initiation and orientation of lamellipodia through adhesion-based signaling. J Cell Biol 208: 443-455.

28. Geuna S, Raimondo S, Fregnan F, Haastert-Talini K, Grothe C (2016) In vitro models for peripheral nerve regeneration. Eur J Neurosci 43: 287-296.

29. Gambarotta G, Pascal D, Ronchi G, Morano M, Jager SB, et al. (2015) Local delivery of the Neuregulin1 receptor ecto-domain (ecto-ErbB4) has a positive effect on regenerated nerve fiber maturation. Gene Ther 22: 901-907.

30. Mooney M, Wrobel S, Ferguson E, Ziv-Polat O, Shahar A, et al. (2014) Nanotechnology versus stem cell engineering: in vitro comparison of neurite inductive potentials. Int J Nanomedicine 9: 5289–5306.

31. Geuna S, Gnavi S, Perroteau I, Tos P, Battiston B (2013) Tissue engineering and peripheral nerve reconstruction: an overview. Int Rev Neurobiol 108: 35–57.

32. Gnavi S, Fornasari BE, Tonda-Turo C, Ciardelli G, Zanetti M, et al. The influence of electrospun fibre size on Schwann cell behaviour and axonal outgrowth. Mater Sci Eng C Mater Biol Appl dii: 629-635.

33. de Ruiter GC, Malessy MJ, Yaszemski MJ, Windebank AJ, Spinner RJ (2009) Designing ideal conduits for peripheral nerve repair. Neurosurg Focus 26: E5.